Utilizing InSAR for Surface Stability Monitoring in Mining Sites: A Case Study of Sukari Gold Mine in Egypt

Bahaa Mohamadi

Institute of Artificial Intelligence, School of Mechanical and Electrical Engineering, Shaoxing University, Shaoxing 312000, China.
– bh.mo@usx.edu.cn

Keywords: Egypt, Mining, PS-InSAR, Sukari Mine, Surface Stability Monitoring.

Abstract

The monitoring of mining sites is crucial as a result of the safety and environmental issues linked to mining activities. Traditional surveying and monitoring tools exhibit limitations in terms of spatial coverage and are associated with various concerns regarding time and cost efficiency. Hence, the mining industry has shown increased interest in the time-series analysis of interferometric synthetic aperture radar (InSAR). This is primarily due to its precision and wide spatial coverage advantages. This study employed an InSAR technology, persistent scatterer interferometry (PSI), to identify potential geohazards within the Sukari gold mine (SGM), located in Egypt. A total of 23 images were collected from the ascending orbit of Sentinel-1 sensor between January 7, 2022, and November 3, 2022, for the SGM mining location. Results revealed relatively stable measurements in non-mining areas of the site, with a surface displacement within ±10mm per year in the line-of-sight (LOS) direction. However, several active mining operation areas showed significant surface motion. Various sections of the open pit of the SGM exhibited displacement, including the southwestern edge (-16.8mm) and the northeastern edge (35.7mm), and the highest velocity was detected at a section of the western edge, which demonstrated an annual displacement of -64mm in the LOS. Additionally, notable surface motion was observed in some parts of the two tailings storage facilities at the site. The results of this study illustrate the importance of InSAR techniques in mining site-wide coverage stability monitoring.

1. Introduction

Surface stability monitoring of mining sites is important to avoid life loss for workers, environmental pollution, and damage to infrastructure and equipment. Especially in open-pit mining sites. Traditional field measurement methods such as total stations, GPS, GNSS, and crack meters lack spatial coverage and have many time and cost-efficiency concerns. In comparison, the timeseries analysis of interferometric synthetic aperture radar (InSAR) has gained more interest in the mining industry in recent years due to its precision measurement, all-weather, all-time data availability, wide spatial coverage, and low cost, thanks to Sentinel-1 data. All those advantages make it possible to detect potential geohazards over the whole mining site in a short time (Haupt et al., 2023; Sun et al., 2023).

Persistent scatterer interferometry (PSI) is a type of microwave remote sensing technique that uses multi-temporal radar images to measure changes in the surface very accurately along the sensor's line of sight (LOS) down to the millimeter level (Ferretti et al., 2001). This technique can detect subsidence, uplift, and horizontal displacements, which are common in mining areas. The availability of space-based SAR sensors allows for frequent monitoring over time, results in semi-real-time monitoring of surface displacement in mining sites, and allows for early detection of small motion. It works as an early warning system for potential geohazards in the event of a gradual increase in surface velocity over time (Sun et al., 2023).

In this study, we utilized PSI to detect surface displacement in the Sukari gold mine (SGM) in Egypt. This mining site is important for the country's economy, with its high annual gold production from estimated reserves exceeding 10 million ounces (Abdelaal et al., 2021). Hence, surface stability monitoring of the site facilities is essential to avoid any mining activity disturbances. Very few studies have utilized InSAR techniques on the SGM site, including Mohamed et al. (2022), which used three-pass D-InSAR to detect ground changes in SGM between September 2017 and September 2018. Another study employed deep recurrent residual U-Net to resolve the unwrapping results of InSAR at the mining site. But without any interest in measuring surface displacement inside the area (Zeyada et al., 2022).

This study used Sentinel-1 (S-1) data acquired in 2022. S-1 is a global acquisition's radar sensor developed and managed by the European Space Agency (ESA) as part of their Copernicus program. S-1 operates in the C-band and provides a spatial resolution of 5m in range and 20m in azimuth directions (Potin et al., 2016). Originally, S-1 consisted of two satellites, Sentinel-1A (S-1A) and Sentinel-1B (S-1B), launched in 2014 and 2016, respectively. However, the failure of S-1B on December 23, 2021, resulted in the availability of S-1A data only since then (Potin et al., 2022).

2. Methodology

2.1. Study Area

Sukari is the largest gold mine in Egypt, covering an area of about 160 km2. SGM is located about 15 km southwest of Marsa Alam City by the Red Sea coast, approximately at 24° 57′ N, 34° 43′ E, in the Eastern Desert of Egypt (Abdelaal et al., 2021; Kriewaldt et al., 2021; Mohamed et al., 2022). It is a historical mining site. Operations at the mining site can be traced back to 5500 years ago, as mining activities were carried out by the Pharaohs, Romans, and Islamic empires (Kriewaldt et al., 2021).

Figure 1 illustrates the mining site of SGM and its main surface contents. The mining operation in Sukari involves open-pit and underground mining processes. The infrastructure of the site includes a processing plant, power generation facilities, a water

https://doi.org/10.5194/isprs-archives-XLVIII-1-2024-523-2024

supply system, and two tailings storage facilities (TSF) (Abdelaal et al., 2021).

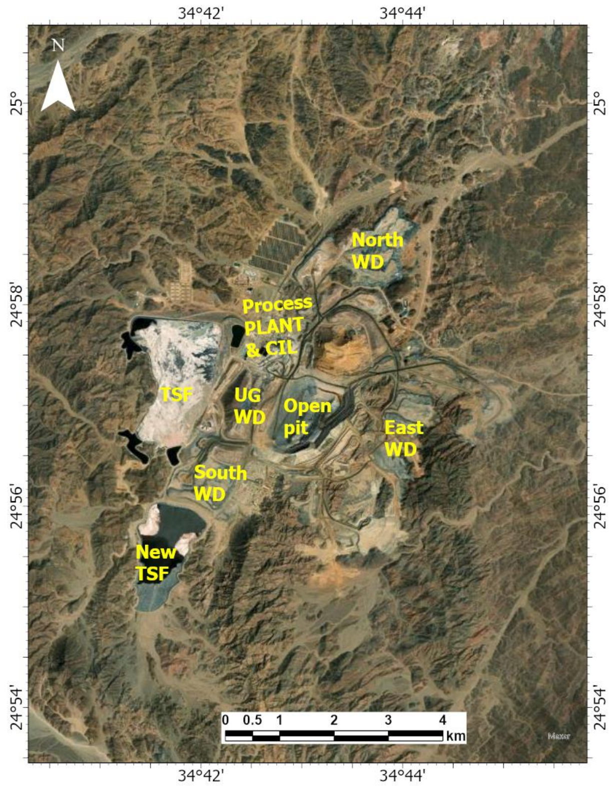

Figure 1. Sukari Gold Mine site. Modified after Abdelaal et al. (2021). WD is a waste dump, and TSF is a tailings storage facility. Base map © ESRI Copyright 2024.

2.2. Data Collection

The analyzed images in this study were acquired from the ascending orbit of S-1. 23 VV-polarization images with dates starting from January 7th, 2022, to November 3rd, 2022, were collected. It is well known that the one-dimensional deformation captured in a single radar's LOS does not fully reflect the characteristics of ground surface displacement at a mining site. Due to the side-looking imaging characteristics of the radar (Sun et al., 2023). However, during this study period, there were no Sentinel-1 images acquired in descending orbit to conduct a full displacement analysis in the area.

2.3. PS-InSAR Processing

Sentinel-1 images were analyzed using SARPROZ software (Perissin et al., 2011) to detect surface displacement at the SGM site by applying the standard PSI technique. In the interferometric analysis, the differential interferometric phase can be described as the following equation (Mohamadi et al., 2019):

$$\Delta\phi_{diff} = \Delta\phi_{defo} + \Delta\phi_{topo} + \Delta\phi_{atmo} + \Delta\phi_{noise} \tag{1}$$

Where $\Delta\phi diff$ = differential interferometric phase
$\Delta\phi defo$ = deformation
$\Delta\phi_{topo}$ = topographic residuals
$\Delta\phi_{atmo}$ = atmospheric delay
$\Delta\phi_{noise}$ = residual noise

PSI exploits the radar signal scattering properties of stable targets, known as persistent scatterers. These targets exhibit strong and stable radar reflections over time, such as buildings, man-made structures, and rocky outcrops (Ferretti et al., 2001). The methodological steps of this study start by selecting appropriate primary images depending on the temporal and spatial baselines of the data (Figure 1). The image acquired on May 7, 2022, was selected as the primary image for this study. The other 22 secondary images were then co-registered with the primary image. To keep the InSAR phase error to 1/100 cycle for Sentinel-1 TOPS acquisition mode, the coregistration accuracy needs to be about 0.0009 samples (Yagüe-Martínez et al., 2016).

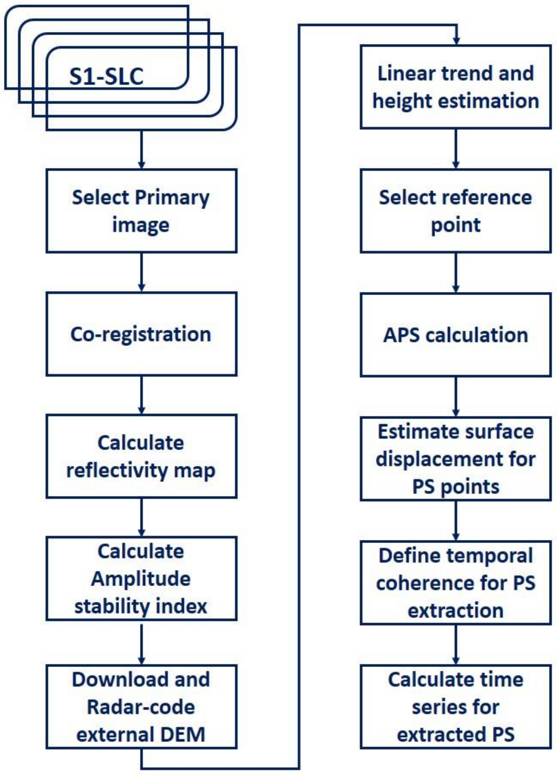

Figure 2. Main steps of PS-InSAR processing in this study

The reflectivity map was calculated from the amplitude of coregistered images, and the amplitude stability index was then estimated to be able to extract persistent scatterers in the study area. Next, a graph network between those permanent scatterers was created to estimate the Atmospheric Phase Screen (APS). It is an important step in the PSI analysis to separate the topographic residuals and the atmospheric delay from the displacement signal (Ferretti et al., 2001). In this study, the linear trend estimation was limited to ±180 mm and the estimation of the residual topographic error to ±225 m to include all areas with significant topographical change in the mining site.

The reference point was also chosen during the estimation of the APS, based on its stability and high temporal coherence over time. Once the APS was estimated, the residual displacement was subsequently determined relative to the chosen reference point. Next, an estimation of the surface displacement was conducted for each PS point in a time series for the full study period. To avoid noisy measurements of moderately coherent points, only points with temporal coherence of 0.7 or above were exported as the final result of surface displacement from the Sukari mining location.

3. Results

Figure 3 shows the annual surface displacement results of PSI analysis in the SGM area. The surface of SGM non-mining areas was found to be stable, with average displacements of ±10mm per year in the radar LOS. The topographic slope at the south of the study area drives a small area of displacement towards the sensor, making it an exception. It showed an annual displacement of about 11.25 mm. A black arrow represents the LOS direction in the results graphs.

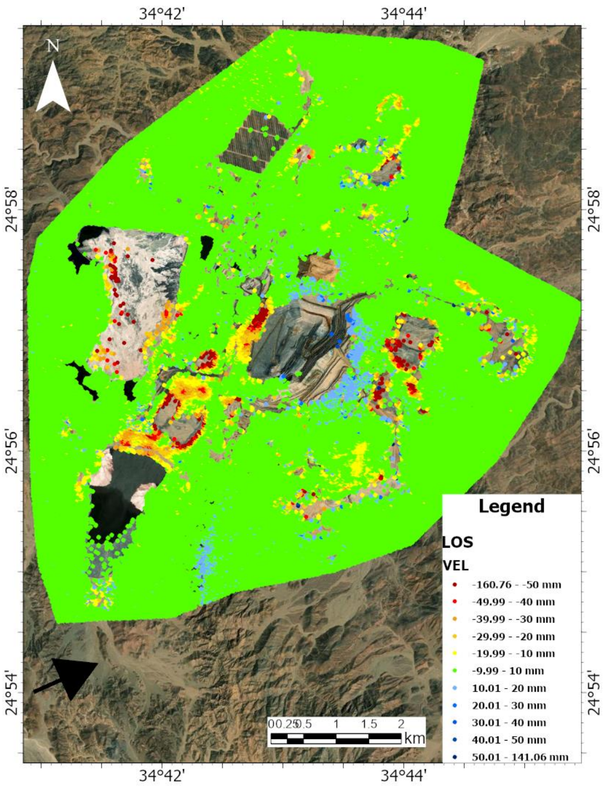

Figure 3. Surface displacement in the Sukari Gold Mine. The black arrow represents the LOS direction.

Areas with intensive mining operations have no PS points, such as large parts of waste dumps, as appears in Figure 3, due to the coherence loss in such areas. Additionally, SAR geometry distortions may result in some gaps in PS distribution in the mining area, especially in the open pit. The following part of the results section will concentrate on areas experiencing active displacement in open pits, TSFs, and waste dumps. As most of the other important facilities of the SGM are relatively stable, including the process plant, which has a displacement average of 1.7 mm per year during the study period.

3.1. Displacement at the Open Pit.

The PSI results of this study show some significant displacement in the SGM’s open pit (Figure 4). The average displacement at the western edge is -27.6mm in the LOS direction. The average displacement increased in a section of the western edge to reach a serious displacement of -64mm per year. On the other hand, the eastern edge of the open pit showed an average displacement of about 12mm towards the sensor. With some PS points, measurement has reached an average displacement of 35.7mm per year at the northeastern edge of the open pit.

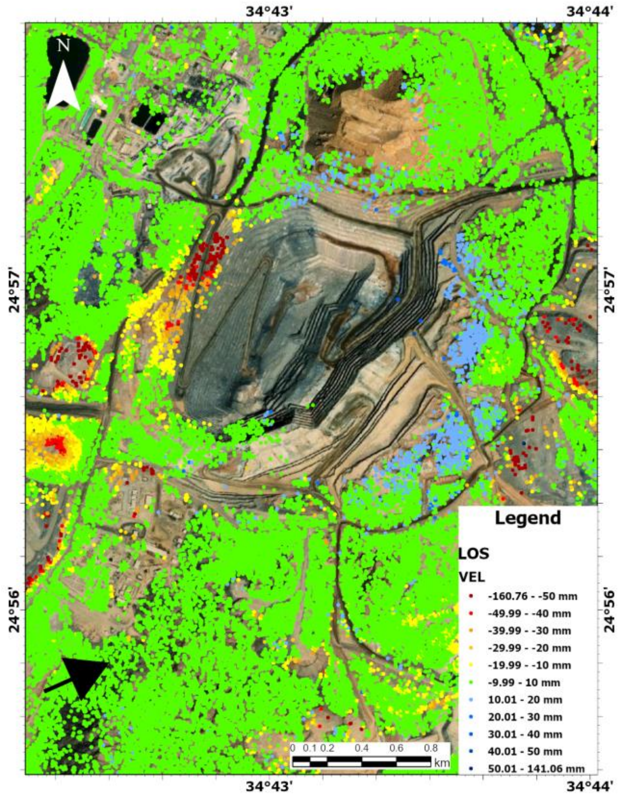

Figure 4. Surface displacement in the SGM’s open pit.

Most of the southern edge of the open pit showed a stable surface with an annual displacement of less than 1mm per year. Except for a small area at the southwest of the open pit with a size of approximately 250 square meters that showed a displacement of -16.8mm. While the northern edge of the open pit showed an annual displacement average of about 11.5mm towards the sensor during the study period.

Figure 5 presents samples of displacement time series at the open pit edges. The first time series sample shows an active and continuous displacement at the western edge of the open pit by an annual average of about -69mm (Figure 5a). Hence, serious investigations have to be done by geotechnical engineers at the site to avoid the collapse of this part. Figure 5b shows a sample of surface displacement from the eastern edge of the open pit. The surface of that sample point remained stable until mid-April 2022. Then, it starts to displace towards the sensor with an annual velocity of more than 30mm.

The northern edge of the open pit exhibited similar behavior as the one at the eastern edge. The surface was stable until May 2022. Then, it started to displace towards the sensor with an annual velocity of about 21mm (Figure 5c). The sample time series at the southern edge was selected from the active area at the south-western part of the open pit (Figure 5d). This sample showed a stable surface status in that area until June 2022. Then, it started to move away from the sensor with an annual velocity average of almost 22 mm. Hence, it is important to continue monitoring the mining site with InSAR techniques to give decision-makers updated information about surface displacement in the open pit so they can make a quick decision in case surface velocity increases overtime.

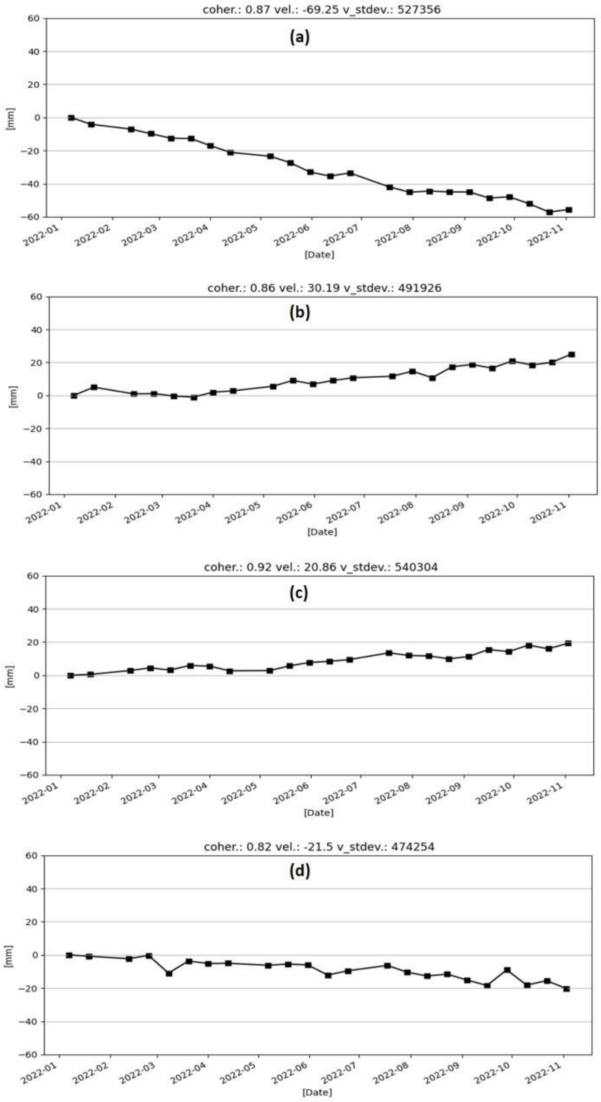

Figure 5. Samples of displacement time series at the open pit edges: (a) sample from the western edge, (b) sample from the eastern edge, (c) sample from the northern edge, and (d) sample from the southern edge.

3.2. Displacement at Tailings Storage Facility (TSFs)

Monitoring TSFs at a mining site is important to avoid any leakage of undesirable chemicals, organic matter, and effluent into the environment. Additionally, with the existence of ground rock, unrecoverable, and uneconomic metals in the TSF, the breakdown of a tailings dam could also result in the mass destruction of site facilities and maybe the loss of lives. By following the Copernicus browser, historical imagery of Sentinel-2 showed that there was one TSF at the west of the mining site until the end of 2020. By the end of 2020, a new TSF emerged to the south of the mining site, and its tailings have been steadily increasing over time.

The original TSF at the west shows sparse points over its area, with an average annual velocity of -30mm in the LOS. The continuous addition of materials to the TSF over time could explain this movement within the TSF area. However, the northwest and central eastern parts of the original TSF edges require careful attention. The average annual velocity of the northwestern and central eastern parts is -40mm and -33mm, respectively.

Regarding the new TSF, no PS points could be detected within the TSF itself due to the liquid contents at the study time (Figure 6). The surface surrounding the new TSF was found to be relatively stable. Except for the northern edge with an average LOS velocity of -20mm per year and some parts of the northwestern edge with an average velocity of -11mm away from the sensor.

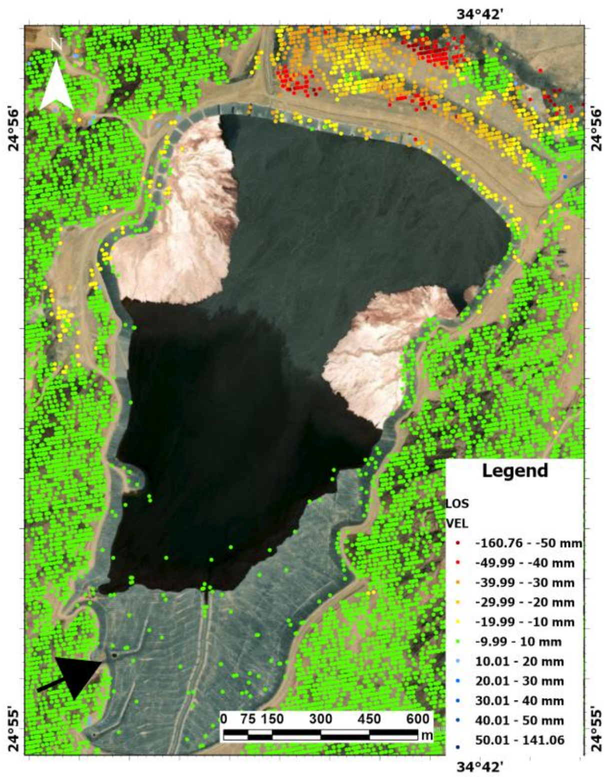

Figure 6. Surface motion at the new TSF of SGM overlayed on a relatively recent ESRI basemap.

By checking the velocity time series at the central northern edge of the new TSF (Figure 7), motion was found to be away from the sensor by an annual average of about -36mm until August 2022. However, the surface seems to have become stable since then. It was suggested that the motion was mostly due to the settelement of the new TSF after construction, affected by the new loads of tailings. Which then reached a stable point in August 2022.

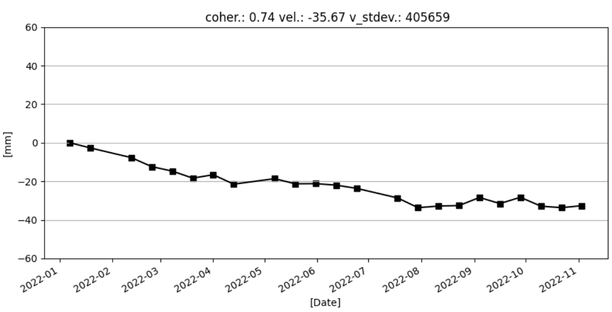

Figure 7. Sample of surface displacement at the central northern edge of SGM's new TSF.

3.3. Displacement at Waste Dumps

Waste dump surfaces at a mining site are always active during mining operations. Hence, it is always expected to lose temporal coherence in most of its parts. Figure 8 illustrates the four main waste dumps of SGM. Large areas of waste dumps lack points, whereas other large parts present sparse points. However, the displacement of surfaces within these areas is normally considered a low level of hazard. The reason behind this consideration is that the location of waste dumps is carefully selected within the site before mining operations start to avoid any possibility of waste or rock falling into important areas of the mine.

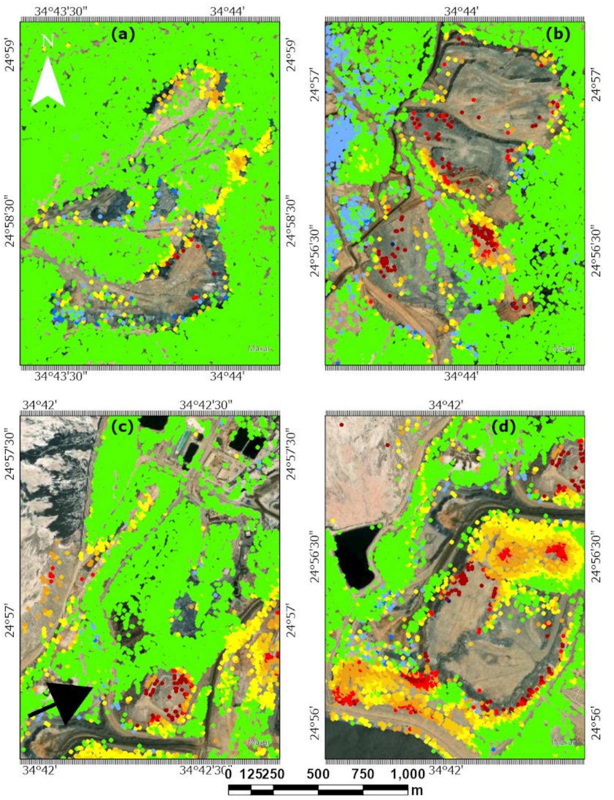

Figure 8. Displacement at the main four waste dumps in SGM: (a) the north waste dump, (b) the east waste dump, (c) the underground mining waste dump, and (d) the south waste dump. The north arrow is presented in white, the LOS direction is presented in black arrow, and the scale bar represents the four maps, and the legend is similar to Figure 6's legend.

Overall, the average velocity of displaced PS points in the north waste dump is -16mm per year (Figure 8a). While the annual average of detected displaced areas in the east waste dump is -32mm in the LOS (Figure 8b). On the other hand, most of the underground waste dump showed stable surfaces except the southern part of it, which reached a high annual velocity average of -49mm away from the sensor. Whereas, the displaced areas of the southeast dump have a maximum velocity of -26mm away from the sensor per year.

4. Conclusion

This study utilized PSI to analyze Sentinel-1 data and assess the potential geohazards in the Sukari gold mine (SGM) in Egypt. It highlighted the advantages of InSAR precise measurements, wide spatial coverage, and relatively low cost, enabling the detection of potential geohazards over the entire mining site. The findings of this study demonstrated general stability in the mountainous area surrounding the mining site, with surface displacements within ±10mm per year. However, significant surface motion was detected in certain areas of the SGM. Especially a section on the western edge of the open pit.

The findings emphasize the importance of continuous monitoring and control of surface stability at mining sites. By utilizing InSAR technology, mining operators can identify areas prone to geohazards and take appropriate measures to mitigate risks. Early detection of surface motion and displacements can serve as an effective warning system, enabling proactive actions to ensure the safety of workers, prevent environmental pollution, and protect critical infrastructure and equipment.

Acknowledgements

The author would like to thank Daniele Perissin for providing the SarProZ software to support this research. The author also acknowledges the use of QuillBot for grammar corrections in this paper.

References

Abdelaal, A., Sultan, M., Elhebiry, M., Krishnamurthy, R.V. and Sturchio, N., 2021. Integrated studies to identify site-specific parameters for environmentally benign mining operations: A case study from the Sukari Gold Mine, Egypt. *Science of the Total Environment*, 750, p.141654; doi.org/10.1016/j.scitotenv.2020.141654.

Ferretti, A., Prati, C. and Rocca, F., 2001. Permanent scatterers in SAR interferometry. *IEEE Transactions on geoscience and remote sensing*, 39(1), pp.8-20; doi.org/10.1109/36.898661.

Haupt, S., Sibolla, B. and Mdakane, L.W., 2023. Time Series Insar Analysis for Slope Stability Monitoring Using SENTINEL-1 in Open Pit Mining. *The International Archives of the Photogrammetry, Remote Sensing and Spatial Information Sciences*, 48, pp.945-951; doi.org/10.5194/isprs-archives-XLVIII-1-W2-2023-945-2023.

Kriewaldt, M., Okasha, H. and Farghally, M., 2021. Sukari Gold Mine: Opportunities and Challenges. *The Geology of the Egyptian Nubian Shield*, pp.577-591; doi.org/10.1007/978-3-030-49771-2_20.

Mohamadi, B., Balz, T. and Younes, A., 2019. A model for complex subsidence causality interpretation based on PS-InSAR cross-heading orbits analysis. *Remote Sensing*, 11(17), p.2014; doi.org/10.3390/rs11172014.

Mohamed, S.A., Nasr, A.H. and Keshk, H.M., 2022. Three-Pass (DInSAR) Ground Change Detection in Sukari Gold Mine, Eastern Desert, Egypt. *In Pervasive Computing and Social Networking: Proceedings of ICPCSN 2021* (pp. 653-662). Springer Singapore; doi.org/10.1007/978-981-16-5640-8_49.

Perissin, D., Wang, Z. and Wang, T., 2011. The SARPROZ InSAR tool for urban subsidence/manmade structure stability monitoring in China. *proceedings of the ISRSE, Sidney, Australia*, 1015.

Potin, P., Rosich, B., Grimont, P., Miranda, N., Shurmer, I., O'Connell, A., Torres, R. and Krassenburg, M., 2016. June.

Sentinel-1 mission status. In Proceedings of EUSAR 2016: *11th European conference on synthetic aperture radar* (pp. 1-6). VDE; doi.org/10.1109/IGARSS.2015.7326401.

Potin, P., Colin, O., Pinheiro, M., Rosich, B., O'Connell, A., Ormston, T., Gratadour, J.B. and Torres, R., 2022, July. Status and Evolution of the Sentinel-1 mission. *In IGARSS 2022-2022 IEEE International Geoscience and Remote Sensing Symposium* (pp. 4707-4710). IEEE; doi.org/ 10.1109/IGARSS46834.2022.9884753.

Sun, D., Deng, W., Yang, T., Li, J. and Zhao, Y., 2023. A Case Study Integrating Numerical Simulation and InSAR Monitoring to Analyze Bedding-Controlled Landslide in Nanfen Open-Pit Mine. *Sustainability*, 15(14), p.11158; doi.org/10.3390/su151411158.

Yagüe-Martínez, N., Prats-Iraola, P., Gonzalez, F.R., Brcic, R., Shau, R., Geudtner, D., Eineder, M. and Bamler, R., 2016. Interferometric processing of Sentinel-1 TOPS data. *IEEE transactions on geoscience and remote sensing*, 54(4), pp.2220-2234; doi.org/10.1109/TGRS.2015.2497902.

Zeyada, H.H., Mostafa, M.S., Ezz, M.M., Nasr, A.H. and Harb, H.M., 2022. Resolving phase unwrapping in interferometric synthetic aperture radar using deep recurrent residual U-Net. *The Egyptian Journal of Remote Sensing and Space Science*, 25(1), pp.1-10; doi.org/10.1016/j.ejrs.2021.12.001